Identification of combinatorial and singular genomic signatures of host adaptation in influenza A H1N1 and H3N2 subtypes

Zeeshan Khaliq[1], Mikael Leijon[2,3], Sándor Belák[3,4], Jan Komorowski[1,5,*]

[1] Department of Cell and Molecular Biology, Computational Biology and Bioinformatics, Science for Life Laboratory, Uppsala University, SE-751 24, Uppsala, Sweden

[2] National Veterinary Institute (SVA), Department of Virology, Parasitology and Immunobiology (VIP)

[3] OIE Collaborating Centre for the Biotechnology-based Diagnosis of Infectious Diseases in Veterinary Medicine, Ulls väg 2B and 26, SE-756 89 Uppsala, Sweden

[4] Swedish University of Agricultural Sciences (SLU), Department of Biomedical Sciences and Veterinary Public Health (BVF)

[5] Institute of Computer Science, Polish Academy of Sciences, 01-248 Warszawa, Poland

* Corresponding Author

Email Addresses:

ZK: zeeshan.khaliq@icm.uu.se

ML: mikael.leijon@sva.se

SB: sandor.belak@slu.se

JK: jan.komorowski@icm.uu.se

Abstract

Background

The underlying strategies used by influenza A viruses (IAVs) to adapt to new hosts while crossing the species barrier are complex and yet to be understood completely. Several studies have been published identifying singular genomic signatures that indicate such a host switch. The complexity of the problem suggested that in addition to the singular signatures, there might be a combinatorial use of such genomic features, in nature, defining adaptation to hosts..

Results

We used computational rule-based modeling to identify combinatorial sets of interacting amino acid (aa) residues in 12 proteins of IAVs of H1N1 and H3N2 subtypes. We built highly accurate rule-based models for each protein that could differentiate between viral aa sequences coming from avian and human hosts, . We found 68 combinations of aa residues associated to host adaptation (HAd) on HA, M1, M2, NP, NS1, NEP, PA, PA-X, PB1 and PB2 proteins of the H1N1 subtype and 24 on M1, M2, NEP, PB1 and PB2 proteins of the H3N2 subtypes. In addition to these combinations, we found 132 novel singular aa signatures distributed among all proteins, including the newly discovered PA-X protein, of both subtypes. We showed that HA, NA, NP, NS1, NEP, PA-X and PA proteins of the H1N1 subtype carry H1N1-specific and HA, NA, PA-X, PA, PB1-F2 and PB1 of the H3N2 subtype carry H3N2-specific HAd signatures. M1, M2, PB1-F2, PB1 and PB2 of H1N1 subtype, in addition to H1N1 signatures, also carry H3N2 signatures. Similarly M1, M2, NP, NS1, NEP and PB2 of H3N2 subtype were shown to carry both H3N2 and H1N1 HAd signatures.

Conclusions

To sum it up, we computationally constructed simple IF-THEN rule-based models that could distinguish between aa sequences of virus particles originating from avian and human hosts. From the rules we identified combinations of aa residues as signatures facilitating the adaptation to specific hosts. The identification of combinatorial aa signatures suggests that the process of adaptation of IAVs to a new host is more complex than previously suggested. The present study provides a basis for further detailed studies with the aim to elucidate the molecular mechanisms providing the foundation for the adaptation process.

Keywords

Influenza A virus, Host specificity, combinatorial signatures, MCFS, Rosetta, Rough sets.

Background

IAVs have been known for a long time to cause disease in a wide range of host species, including humans and various animals. The IAVs are zoonotic pathogens that can infect a broad range of animals from birds to pigs and humans. The interspecies transmission requires that IAVs adapt to the new host and the whole process is facilitated by their high mutation rates [1]. This can result in epidemics and pandemics with severe consequences for both human and animal life. In addition to the yearly epidemics that has proved fatal for at least 250,000 humans worldwide, in the 20th century alone [2], there has been at least five major pandemics; the Spanish flu of 1918, Asian influenza of 1957, Hong Kong influenza of 1968, the age restricted milder Russian flu of the 1977 [3, 4] and the Swine flu of 2009. Thus, new flu epidemics and pandemics are a constant threat. Given our poor understanding of the

HAd process of the virus, which can be a major factor for such epidemics and pandemics, it is very hard to predict the type of the virus that will cause the coming outbreaks.

The IAVs are usually classified into subgroups based on the two surface glycol-proteins, hemagglutinin (HA) and neuraminidase (NA). To date, 18 types of HA (H1-H18) and 11 types of NA (N1-N11) are known [5-7]. Most of these species have wild birds as their natural hosts. IAVs are usually adapted and relatively restricted to a single host but occasionally the virus can jump and adapt to a new host species. This cross of the species barrier is proved by the pandemic H1N1, H3N2, H2N2 and the most recent H5N1 and H7N9 subtype outbreaks, which are thought to have evolved from avian or porcine sources [8, 9, 5].

The HA protein plays a crucial part in defining the adaptation of the virus to different hosts since it binds to the receptor providing the entry into host cells. The avian strains of the IAVs are known to prefer a receptor with α2,3-sialic acid linkages while the human strains have a preference for a receptor with α2,6-sialic acid linkages [10]. However, other proteins such as the polymerase subunits have also previously been shown to play a role in the adaptation of IAVs to different hosts [11, 12].

Computational methods, like artificial neural networks, support vector machines and random forests, have been used previously to predict hosts of IAVs [13-15]. Furthermore, several other studies have previously been carried out predicting genomic signatures specifying different hosts, both computationally and experimentally [16-22]. Amino acid changes taken one at a time, i.e. singular aa changes), in viral protein sequences between different hosts have been reported by these studies as host-specific signatures, either directly or indirectly facilitating the HAd process. Despite these findings, this process of adaptation of IAVs in different

hosts is still not completely understood. Given the complex nature of the problem we suspected that the HAd signatures are not necessarily univariate. Essentially, in addition to the proven effects of singular aa residues, there might be a combinatorial use of aa residues in nature that affect the adaptation of IAVs to new hosts.

To this end, for both H1N1 and H3N2 subtypes, we analyzed aa sequences of 12 proteins expressed by the viruses. We built high quality rule-based models, based on rough sets [23], for each of the 12 proteins, predicting hosts from protein sequences. The models consisted of simple IF-THEN rules that lend themselves to easy interpretation. The combinations of aa residues used by the rules were identified as HAd signatures. In additions to such combinatorial signatures, novel singular signatures were also identified from the rules. The singular and, especially, the combinatorial signatures provide novel insights into the complex HAd process of the IAVs.

Results

Feature selection reduces the number of features needed to discern between hosts

Monte Carlo Feature Selection (MCFS) [24]was used to obtain a ranked list of significant features, here significantly informative aa positions in all the proteins for both subtypes, that best discern between the hosts. This step helped us remove any kind of noise that could have been in the data. More importantly, the use of MCFS considerably reduced the number of aa positions to be analyzed further, as shown in Table 1. The HA protein had 628 positions to start with and after running MCFS on the data, we were left with 115 and 88 positions for H1N1 and H3N2 subtypes,

respectively (81.7% and 86% reduction in the number aa positions). On average there was a 79.8% reduction in the number of aa positions across all the proteins for H1N1 subtype and 82.8% for the H3N2 subtype (Table 1). Only the significant features were used for further analysis in this study. The ranked lists of the significant features are provided as a supplementary file (see Additional file 1).

Rule-based models for each protein

Since the number of sequences belonging to human and avian hosts were not balanced in the training data of either subtype (Table 1), we balanced the data sets by a method called under-sampling, as described in detail in Methods. For data sets of each protein and each subtype we created 100 under-sampled subsets. Each of these subsets was used to build a classifier, consisting of IF-THEN rules, whose performance was assessed by a 10-fold cross-validation. Mean accuracies of the 100 classifiers were averaged and shown in Figure 1. HA classifiers for H1N1 and non-structural protein 1 (NS1) classifiers for H3N2 subtypes were the best ones with a mean accuracy of 98% and 98.9%, respectively. Nuclear export protein (NEP) classifiers of the H1N1 subtype and matrix protein 1 (M1) classifiers of the H3N2 subtype had lowest mean accuracy of 83.4% and 88.8%, respectively, which is still a very good result.

For each protein of each subtype a single rule-based model containing only the most significant rules from their respective 100 classifiers was inferred (Methods). We then reclassified the training data of each protein with its respective rule-based model to get an idea of its performance in terms of classification of human and avian sequences. Polymerase acidic protein X (PA-X), which is a frame-shift product of the third RNA segment, HA and NEP (NS2) models performed the best (Mathew's correlation coefficient (MCC) = 1, MCC = 0.99, MCC = 0.99, respectively) among the H3N2 models while HA, NA and NS1 models performed the best among the

H1N1 models (MCC = 0.96, MCC = 0.95, MCC = 0.95, respectively) (Figure 2). The poorest of the H1N1 models was the PA-X protein model (MCC = 0.86) and of the H3N2 models was the polymerase basic protein F2 (PB1-F2) protein model (MCC = 0.86). The complete HA H1N1 rule-based model is shown in Table 2. Models for the remaining proteins for both subtypes are provided as supplementary material (Additional file 2).

To further verify the validity of the rule-based models created, we tested them on new, unseen data. This data was protein sequences published at the NCBI resource between 30th of November 2014 and 16th of April 2015. For the H1N1 subtype, the rule-based models of M1, nucleoprotein (NP), NS1, NEP (also called non-structural protein 2 (NS2)), PB1-F2, polymerase basic protein 1 (PB1) and polymerase basic protein 2 (PB2) provided perfect classification (i.e. all the sequences were correctly classified). For the H3N2 subtype data, the models of HA, M1, NP, NS1, NEP (NS2), polymerase acidic protein (PA), PB1 and PB2 also gave a perfect classification. Table 3 shows the performance of all rule-based models on the unseen data. A list of names of the viruses that could not be classified or were miss-classified for both subtypes is given in Additional file 3.

Predicted signatures of HAd

The rule-based models allowed us to further interpret them and see how they differentiated viral avian from viral human sequences. Each of the models was analyzed separately for HAd signatures. The constituent rules of a model associated aa residues at specific positions with an avian or human host. The confidence in these associations is shown as the accuracy, support and the decision coverage shown in the rule-based models. For the combinations in our models we also calculated a combinatorial accuracy gain (CAG), which is the percentage points gain in accuracy

of the combination as compared to the average of the accuracies of its constituent singular conditions when taken independently.

Combinatorial signatures

As expected we found aa combinations in HA, M1, matrix protein 2 (M2), NP, NS1, NEP (NS2), PA, PA-X, PB1 and PB2 proteins to be associated with specific hosts in the H1N1 subtype. In the H3N2 subtype, we found combinations in M1, M2, NEP, PB1 and PB2 proteins. A complete set of combinations for both subtypes is given in a supplementary file (see Additional file 4: Combinations_from_rules). Ciruvis diagrams [25] for visualization of combinations of interacting amino acids were used to illustrate the cases of three or more combinations in the models of both subtypes associated with the avian hosts (see Figure 3 and Figure 4).

Residues 14G of the M2 H1N1 model and 82N of the PB2 H3N2 model were the most connected ones interacting with six other aa residues each. Amino acid residues having interactions with more than one other residue, in both the subtypes are listed in Table 4. These strongly interacting residues might be relatively more essential to HAd than the less connected ones.

Singular (linear) signatures

Previous studies [16-22] mostly found the adaptation signatures on the internal proteins and did not look into surface glycoproteins (HA and NA). In contrast, we found singular signatures on all the proteins of both subtypes, including the HA, NA and the newly discovered PA-X proteins. PA-X protein shares the human signature 85I with PA in the H1N1 model while it shares human signatures 28L and avian signature 28P in the H3N2 models. In total, 189 singular signatures were found, in both subtypes combined. Out of these, 132 signatures were novel and not reported by

192 the previous studies (Table 5). A complete list of singular signatures is given in the
193 supplementary material (see Additional file 4: singletons_H3N2, singletons_H1N1)

194 **Specific aa changes associated with HAd**

195 Some of the rules from our models associated different residues at the same aa
196 positions with avian and human hosts. This can be seen as a mutation (aa change)
197 associated to the adaptation of the viral proteins to a specific host. Eight mutations
198 were found for the H1N1 subtype and 10 for the H3N2 one. In the H1N1 subtype,
199 mutations F6V in HA, P46T and L74V in NA, I6M in both NS1 and NEP and L58- in
200 PB1-F2 were novel. In the H3N2 subtype, mutations R78E in HA, A30I, N40Y and
201 I44S in NA, P28L and R57Q in PA and P28L in PA-X were not identified in the
202 previous studies. Table 6 shows all such mutations in both subtypes.

203 **Predicted signatures are not specific to sub-clades of the strains**

204 The support and the decision coverage of the rules showed whether the aa signatures
205 identified were specific to sub-clades or were more general i.e. spread out across the
206 sub-clades. The higher decision coverage indicated more generality of the rule. For
207 example, the top five rules for the avian class have the following very high decision
208 coverage: rule1 – 98.5%, rule2 – 98.5%, rule3 – 97.8%, rule4 – 98.5% and rule5 –
209 97.8%. It follows that the rules are general. To further illustrate this generality, and
210 to show the diversity in our training data set, a phylogenetic analysis was carried out
211 (additional file 5). Top five rules specifying each host were mapped onto the created
212 phylogenetic trees, separately for each host, for all the proteins of both subtypes.
213 As an example, consider the avian PB2 H3N2 tree (Figure 5). 91.4% of the
214 sequences are covered by rule 1, 2, 3, 4 and 5, which is illustrated by the violet
215 coloring of the leaves in the tree. Only, 1.4% of the sequences are not covered by

rule4, yet they are covered by rule 1, 2, 3, and 5, and similarly for the remaining coverage. For the corresponding human tree, the figures are 89.3% coverage for the top five human rules. One can see that this generality prevails in all other proteins.

Validity of HAd signatures across H1N1 and H3N2 subtypes

To see whether the signatures associated with HAd identified in the H1N1 subtype could also function as signatures for the H3N2 subtype and vice versa, we classified H3N2 subtype data with H1N1 models and H1N1 subtype data with H3N2 models. Good classifications meant that the rules (and consequently the signatures associated to adaptation) generated for one subtype were valid for the other one. Bad classifications meant that the rules of one subtype did not hold for the data of the other subtype and hence no cross-subtype marker validity. Both HA and NA H1N1 models were bad classifiers for the HA and NA of the H3N2 type data, respectively since they failed to distinguish avian sequences in the data in both cases (Sp = 0) (Table 7). It should be kept in mind that the outcome *human* was considered positive outcome and the outcome *avian* considered as a negative one. The PA-X H1N1 model could not recognize human sequences in the PA-X H3N2 data (Sn = 0). Furthermore, the models of PA, PB1-F2 and PB1 proteins of H1N1 subtype were bad classifiers of the H3N2 data (MCC = -0.11, MCC = 0.056, MCC = 0.302), specifically failing to identify sequences coming from human hosts (Sn = 0.021, Sn = 0.023, Sn = 0.563). This meant that H1N1 HAd signatures in the models of HA, NA, PA-X, PA, PB1-F2 and PB1 proteins were not valid for H3N2 subtype data and these proteins of the H3N2 subtype carried only H3N2-specific HAd signatures. Contrary to this, the H1N1 models of M1, M2, NP, NS1, NEP and PB2 proteins were able to distinguish between H3N2 subtype sequences coming from avian and human sources reasonably well (Sn = 0.97–1.0; Sp = 0.64–0.94; MCC = 0.776–0.941). It proved that these

proteins of the H3N2 subtype, in addition to the stronger H3N2 HAd signatures, also carried H1N1 HAd signatures.

The H3N2 models of HA, NA, NP, NS1, NEP, PA-X and PA proteins could not classify avian and human sequences of H1N1 subtype correctly (MCC = -0.004–0.251). This means that these proteins of the H1N1 subtype carried H1N1-specific signatures. Whereas the successful classifications of H1N1 subtype data of M1, M2, PB1-F2, PB1 and PB2 proteins by the respective H3N2 models (MCC = 0.788–0.888; Sn = 0.956–0.992; Sp = 0.766–0.951) proved that these H1N1 proteins carried both H1N1 and H3N2 signatures.

Discussion

In this study we have focused on H1N1 and H3N2 and restricted our analyses to these two subtypes. Our models performed reasonably well since all of them had an average accuracy of more than 90% in the 10-fold cross validation except NEP (NS2), M1 and M2 protein models of the H1N1 type (Accuracy: 83.4%, 87.7% and 87.6%, respectively) and M1 protein model of the H3N2 type (Accuracy 88.8%) (Figure 1). The reason for the relatively low accuracies of the above exceptions could be either the lack of training sequences from which the models learn or these sequences may lack stronger genomic signatures specific to hosts.

In previous studies [16-22], signatures of adaptation were mostly found on the internal proteins, especially in viral ribonucleoprotein complexes consisting of viral polymerases and NP. The fact that we were able to build high quality models for all the proteins for both subtypes, indicated that all the proteins, including the highly variable HA and NA proteins and the recently discovered PA-X protein, carry genomic signatures specific to hosts. A major difference between our models and the

ones previously reported is that the previous models were black box classifiers whereas our models are transparent. Black box classifiers give classification but do not provide any straightforward possibility to identify which parameters and for which values a classification is obtained. Transparent classifiers allow explicit analysis of the model, i.e. the features and their values, for each classified object. The models created in this study used aa positions as features and aa residues at those positions as the values for those features, hence lending themselves for easy interpretation and further analysis.

Previous studies listed above reported only on singular aa positions as HAd signatures. However, in addition to singular aa positions, we also identified combinations of aa residues at specific positions as HAd signatures. This is the very first time that combinations of aa positions are reported in this context. These combinations are shown as conjunctive rules, i.e., rules with more than one condition in the IF part. It appeared that some aa residues were part of more than one combination in our models. This may suggest that these residues are relatively more important in establishing HAd then the ones appearing in one combination only (Table 4).

In the M2 H1N1 model, the combinations associated with avian hosts had a Glycine (G) residue at position 14 while the combinations for human hosts had a Glutamic acid (E) in the same position. Similarly, in PB2 H3N2 model, Arginine (R) at position 340 was associated to avian hosts while Lysine (K) residue at the same position to human hosts. It seems that the mutations G14E in M2 H1N1 and R340K in PB2 H3N2 model facilitate the shift of hosts from avian to human. However, these residues always appear in combination with other residues and therefore they cannot be used in forms other than the combinations themselves. The reason is obvious. The

confidence measures (accuracy, support and decision-coverage) were calculated for the combination as a whole. We do not report such mutations in our list of mutations affecting HAd although they indicate an effect. The functions of these combinations at a molecular level are not understood yet, but they provide a novel and interesting perspective of looking at sequence based HAd signatures.

HA and NA of both subtypes were found to be only carrying subtype-specific signatures. This goes well with the current knowledge that these two proteins are the most diverse proteins that are specifically adapted to interact with the host cell. M1, M2 and PB2 are shown to be the most conserved proteins from the point of view of host specifying genomic signatures since they carried the host signatures valid for both subtypes.

The signatures found in this study were also considered in other contexts in other studies such as viral viability and antiviral resistances. For instance, positions 30, 142, 207 and 209 occurring in the H1N1 M1 models have been previously shown to affect viral production when mutated [26], while mutation S31N derived from M2 models is a known marker of amantadine resistance [27-30]. Table 8 lists all the aa residues and their descriptions as found in different contexts in the literature. All these different contexts, that the aa residues from our models are described in, show that they affect the fitness of the viruses in one or the other way, which in turn facilitates their adaptation to the new environment or hosts.

Conclusions

The highly predictive rule-based models built for 12 proteins for H1N1 and H3N2 subtypes suggest that there are HAd signatures on all the protein including the diverse HA, NA and the newly discovered PA-X protein that were not previously studied in

this context. In addition, the transparent nature of our method allowed us to further investigate our models for how the predictions are actually done. This resulted in a list of aa residues and their combinations associated with host specifity. Some of the aa residues identified in this study were already known while others are novel. The ability of our methods to capture the combinatorial nature of the HAd process makes this study unique in its nature. We discovered that the surface proteins HA and NA carry subtype-specific host signatures in both subtypes while NP, NS1, NEP, PA-X and PA of the H1N1 subtype and PA-X, PA, PB1-F2 and PB1 of the H3N2 subtype carry subtype-specific host signatures. We showed that M1, M2, PB1-F2, PB1 and PB2 of the H1N1 subtype carried H1N1 and some additional H3N2 signatures, and vice versa, M1, M2, NP, NS1, NEP and PB2 of the H3N2 subtype carried H3N2 and some additional H1N1 host signatures. The computational results presented here will eventually require further analysis by testing the host-pathogen interactions under laboratory conditions. We believe that the computational analyses provide important support in the characterization of host-pathogen interactions and the proper combination of *in silico* and *in vitro* (probably even *in vivo*) studies will yield important novel information concerning the infection biology of various viruses and other infectious agents.

Methods

The combined feature selection – rule-based modeling methodology used in this is similar to our previous work where we identified a complete map of potential pathogenicity markers in the H5N1 subtype of the avian influenza A viruses [31].

Data

The data used to make the models was downloaded from the NCBI flu database found at http://www.ncbi.nlm.nih.gov/genomes/FLU/Database/nph-select.cgi?go=database [32]. Full-length plus (nearly complete, may only miss the start and stop codons) protein sequences of the twelve proteins namely, HA, NA, NP, M1, M2, NS1, NEP (NS2), PA, PA-X, PB1, PB2 and PB1-F2, were separately downloaded as published up till November 30, 2014. Identical sequences were represented by the oldest sequence in the database. For each protein, sequences of the H3N2 and H1N1 subtypes of avian and human hosts were downloaded. Sequences of the mixed subtypes were not included in this study. Table 1 shows the number of sequences for each of the proteins for each subtype. For each protein we combined the sequences of the two subtypes used in this study into a single file and aligned them with MUSCLE (v3.8.31) [33].

Decision Tables

A decision table was created for each of the proteins for both the subtypes. A decision table can be seen as a tabularized form of the aligned FASTA sequences with an extra decision/label column, which in our case was the host information. The first column of the decision tables contained the identifier of the sequence, and the last column was the label/outcome column, the host information in our case and the rest of the columns represented the sequence information corresponding to the aligned FASTA files. The alignment gaps were represented by a '?' in the decision tables. The rows of a decision table were called objects each representing a particular aa sequence and a label. Columns other than the first and the last one were the features.

Feature selection

MCFS, as described in [24], was used to rank the features of the decision tables with respect to their ability to discern between avian and human hosts. MCFS is implemented as a software package dmLab [34]. MCFS uses a large number of decision trees and assigns a normalized relative importance (RI-norm) score to each feature such that the features contributing more to the discernibility of the outcome gets a higher score. Statistical significance of the RI-norm scores was assessed with a permutation test and significant features ($p<0.05$), after Bonferroni correction [35], were kept as described in [36]. Only these features were used in the further rule-based model generation.

Under-sampling the data sets

In the training data for both subtypes, the number of sequences from human hosts was considerably higher than that from the avian hosts. It has previously been shown that this imbalance affects the learning in favor of the dominating class [37]. However to address this problem one can artificially balance the classes [38]. To this end, a technique called under-sampling was used where the sequences belonging to the dominating class were randomly sampled equal to the class having the lesser number of sequences and repeated this step 100 times. In this way for each protein and for each subtype we created 100 subsets where the number of sequences belonging to human and avian hosts were equal. A single rule-based classifier was inferred from each of the subsets, which resulted in 200 classifiers per protein. We illustrate the process with the following example.

The data set of the NA protein of the H1N1 subtype had 3093 human and 205 avian sequences, which was a significant imbalance in the number of sequences. From the

human set we created subsets by randomly extracting 100 times 205 human sequences and joining them with the 205 avian sequences to create 100 subsets.

Rough sets and rule-based model generation

Rough set theory [23] was used to produce minimal sets of features that can discern between the objects belonging to different decision classes. ROSETTA [39], a publicly available software system that implements rough sets theory, was used to transform the minimal sets of features into rule-based models [40] that consisted of simple IF-THEN rules. A complete description of rough sets can be found in [41] and the combined MCFS-ROSETTA approach to model generation in bioinformatics is described in [42].

The input data to ROSETTA were the balanced decision tables created in the previous step with only the significant features obtained from applying MCFS. ROSETTA computed approximately minimal subsets of feature combinations that discerned between avian and human hosts with the Johnsons algorithm implemented in ROSETTA. The classifiers were collections of IF-THEN rules. A sample rule from the HA-H1N1 model:

Rule	Accuracy (%)	Support	Decision Coverage(%)
IF P200=P AND P222=K THEN host=Avian	91.3	229	97.7

reads as: **"IF** *at position 200 there is a Proline residue* **AND** *at position 222 there is a Lysine residue* **THEN** *the sequence is from an avian host***"**.

There is additional information about the rules available. *Support* is the set of sequences (229 sequences) that satisfy the conditions of the left hand side (LHS), i.e. the set of sequences that have a proline residue at position 200 and a lysine residue at position 222. For this rule, *Accuracy* is 91.3% that is the proportion of correctly

406 classified sequences to the total number of supporting sequences (209/229). Human
407 sequences are considered positive and avian as negatives in this study. The decision
408 coverage for this rule is 97.7%, which means it correctly classifies 97.7% of the total
409 avian sequences used to train the classifier. It is calculated as follows:

$$Decision\ Coverage\ (\%) = \left(\frac{Accuracy \times Support}{Total\ training\ objects\ of\ the\ decision\ class}\right) \times 100$$

410 $Accuracy \times Support$ gives us the total number of sequences that are correctly
411 classified by the rule. Since the rule is for the avian decision class, the total number of
412 avian sequences used to train the classifier was 214. So for the stated rule the decision
413 coverage will be ((0.913*229)/214)*100, which is equal to 97.7%. The above rule is a
414 conjunctive rule since there is a conjunction of conditions (`P200=P AND P222=K`)
415 in the left hand side (LHS) of the rule. A conjunctive rule captures the underlying
416 combinatorial nature of the HAd process. Each conjunctive rule must always be used
417 as combination only, because the support, accuracy and the decision coverage
418 measures are calculated for the conjunction and not for the individual conjuncts. A
419 rule can also be a singleton rule where LHS consists of only a single condition.
420 The confidence in these classifiers come from the 10-fold cross validation performed
421 in ROSETTA. In a 10-fold cross validation step the input data set is randomly divided
422 into ten equal subsets, say {P1, …, P10}. A classifier is trained on the first nine
423 subsets {P1, …, P9} and then tested on the remaining, P10 subset. In the next run,
424 another classifier is trained on {P1, …, P8, P10} and its performance is tested on the
425 remaining subset, this time P9. Notice that each time the test set is a different one.
426 The process is repeated 10 times and by then each subset has been used once as a test
427 set. The performance of all the classifiers is averaged and presented as a cross-
428 validation accuracy. Such a validation is quite common in machine learning since one

becomes more or less assured that the performance of the classifier was not simply by chance.

Extraction of a single rule-based model for each protein

Rules from all the 100 classifiers were combined into a single file. Duplicates were removed. Among partially identical rules, the one with the highest decision coverage was kept. If the difference of decision coverage was lower than 1% then the shortest (the rule with least conditions) was kept. Accuracy, support and decision coverage were calculated on the complete data set for all the rules. Rules that were below the 90% accuracy and 30% decision coverage thresholds were discarded. In this way we extracted a single, high quality rule-based model for each of the protein for both H1N1 and H3N2 subtype data.

Classification of sequences

In order to classify a sequence, each rule from the model was applied on it. If the conditions of the rule matched the sequence, the rule was said to fire on the sequence. Every fired rule voted for a particular classification specified by its THEN-part. The number of votes a fired rule casted was the accuracy multiplied by the support of the rule. For a sequence several rules may fire, each casting votes in favor of the class in the THEN-part. The final classification was assigned based on the majority of votes.

Consider the rules:

In case of 1) IF P70=S THEN host=Avian. Acc=94.0% Supp=50

2) IF P14=M and P32=I THEN host=Avian. Acc=93.0% Supp=43

3) IF P14=L THEN host=Human. Acc=100% Supp=285

4) IF P57=L THEN host=Human. Acc=100% Supp=273

Now let us assume that these four rules are applied to a sequence an it turns out that Rule 2, 3 and 4 fire for this sequence. Rule 2 will cast 40 (0.93*43) votes for class Avian while rule 2 and rule 3 will cast 285 and 273 votes in favor of class Human. So, the sequence will be classified as class Human since the number of votes is 558 versus 40.

In case of no rules fired or there was a tie in the votes, the sequences were labeled as unknown.

Performance evaluation statistics of the rule-based models

In this study the outcome *human* was considered as a positive outcome and outcome *avian* was considered as a negative one. True positives (TP) were sequences correctly classified as coming from human hosts. True negatives (TN) were sequences correctly classified as coming from avian hosts. False positives (FP) were actually avian sequences but incorrectly classified as human sequences and false negatives (FN) were actually human sequences that were incorrectly classified as avian sequences. The performance of the models for all the proteins for both H1N1 and H3N2 was assessed by the following statistics.

Sensitivity: it is also known as the true positive rate (TPR). In our case, rate at which a model correctly identifies sequences coming from a human host is the sensitivity i.e. a sequence originally from human host and classified as coming from human hosts by the model. It is calculated with the following formula:

$$Sensitivity\ (Sn) = \frac{TP}{(TP + FN)}$$

Specificity: Also known as the true negative rate (TNR). The rate at which the model correctly identifies avian sequences is the specificity, which is calculated by:

$$Specificity\ (Sp) = \frac{TN}{(FP + TN)}$$

Mathew's correlation coefficient: It is a measure of how well a model classifies as a whole. The difference with accuracy is that unlike accuracy Mathew's correlation coefficient is not effected by un-balanced data and hence gives a better overall idea of how well the model is classifying. It is calculated by the following formula:

$$Mathews\ correlation\ coefficient\ (MCC) = \frac{(TP \times TN) - (FP \times FN)}{\sqrt{(TP + FP) \times (TP + FN) \times (TN + FP) \times (TN + FN)}}$$

From alignment positions to true positions

In this study the aa positions for all the H3N2 proteins except the PB1-F2 corresponds to the positions of the *A/Victoria/JY2/1968* virus. For all but PB1-F2 proteins of the H1N1 data, the positions shown in this study correspond to positions on the *A/Wisconsin/301/1976* virus. The PB1-F2 protein for both viruses is in a truncated form and we wanted to show positions from a full-length protein. For this reason we mapped the PB1-F2 H3N2 positions to the PB1-F2 of the *A/New York/674/1995* virus and the PB1-F2 H1N1 positions to full-length PB1-F2 of the *A/duck/Korea/372/2009* virus.

Phylogenetic analysis

FastTree 2.1.8 [43] was used to create the phylogeny trees.

Scripting programming language

Python was used for scripting purposes.

List of abbreviations

aa: Amino acids

CAG: Combinatorial accuracy gain

HA: Hemagglutinin

IAVs: Influenza A viruses

LHS: Left hand side

M1: Matrix protein 1

M2: Matrix protein 2

MCC: Mathew's correlation coefficient

MCFS: Monte carlo feature selection

NA: Neuraminidase

NEP: Nuclear export protein

NP: Nucleoprotein

NS1: Non structural protein 1

NS2: Non structural protein 2

PA: Polymerase acidic protein

PB1: Polymerase basic protein 1

PB2: Polymerase basic protein 2

Sn: Sensitivity

Sp: Specificity

Competing interests

We have no competing interests.

Authors Contribution

ZK has performed all computational experiments and together with JK was the main contributor to the paper. MK and SB have contributed the idea to analyze the virus data following the earlier work of JK. They contributed to writing the paper. JK provided the computational methods, supervised the work and together with ZK was the main contributor to the paper.

Acknowledgements

We would like to thank Husen Umer who provided valuable comments during various stages of the work.

This research was supported by Uppsala University, Sweden, the ESSENCE grant, (ZK and JK), JK was supported in part by Institute of Computer Science, Polish Academy of Sciences, Poland. The EMIDA ERA-NET FP7 EU projects Epi-SEQ (nr. 219235), NADIV (nr. ID 108), the SLU Award of Excellence provided support to SB, and the Swedish Research Council FORMAS Strong Research Environments project, nr 2011-1692, “BioBridges”) to ML and SB.

References

1. Shi Y, Wu Y, Zhang W, Qi J, Gao GF. Enabling the 'host jump': structural determinants of receptor-binding specificity in influenza A viruses. Nature reviews Microbiology. 2014;12(12):822-31. doi:10.1038/nrmicro3362.

2. cdc. Influenza (Seasonal) Fact Sheet. 2014. http://www.who.int/mediacentre/factsheets/fs211/en/. Accessed 17 April 2015.

3. Taubenberger JK, Morens DM. Pandemic influenza--including a risk assessment of H5N1. Revue scientifique et technique. 2009;28(1):187-202.

4. Kilbourne ED. Influenza pandemics of the 20th century. Emerging infectious diseases. 2006;12(1):9-14. doi:10.3201/eid1201.051254.

5. Gamblin SJ, Skehel JJ. Influenza hemagglutinin and neuraminidase membrane glycoproteins. The Journal of biological chemistry. 2010;285(37):28403-9. doi:10.1074/jbc.R110.129809.

6. Tong S, Li Y, Rivailler P, Conrardy C, Castillo DA, Chen LM et al. A distinct lineage of influenza A virus from bats. Proceedings of the National Academy of Sciences of the United States of America. 2012;109(11):4269-74. doi:10.1073/pnas.1116200109.

545 7. Tong S, Zhu X, Li Y, Shi M, Zhang J, Bourgeois M et al. New world bats harbor
546 diverse influenza A viruses. PLoS pathogens. 2013;9(10):e1003657.
547 doi:10.1371/journal.ppat.1003657.

548 8. Reid AH, Fanning TG, Hultin JV, Taubenberger JK. Origin and evolution of the
549 1918 "Spanish" influenza virus hemagglutinin gene. Proceedings of the National
550 Academy of Sciences of the United States of America. 1999;96(4):1651-6.

551 9. Garten RJ, Davis CT, Russell CA, Shu B, Lindstrom S, Balish A et al. Antigenic
552 and genetic characteristics of swine-origin 2009 A(H1N1) influenza viruses
553 circulating in humans. Science. 2009;325(5937):197-201.
554 doi:10.1126/science.1176225.

555 10. Matrosovich MN, Gambaryan AS, Teneberg S, Piskarev VE, Yamnikova SS,
556 Lvov DK et al. Avian influenza A viruses differ from human viruses by recognition of
557 sialyloligosaccharides and gangliosides and by a higher conservation of the HA
558 receptor-binding site. Virology. 1997;233(1):224-34. doi:10.1006/viro.1997.8580.

559 11. Li OT, Chan MC, Leung CS, Chan RW, Guan Y, Nicholls JM et al. Full factorial
560 analysis of mammalian and avian influenza polymerase subunits suggests a role of an
561 efficient polymerase for virus adaptation. PloS one. 2009;4(5):e5658.
562 doi:10.1371/journal.pone.0005658.

563 12. Subbarao EK, London W, Murphy BR. A single amino acid in the PB2 gene of
564 influenza A virus is a determinant of host range. Journal of virology.
565 1993;67(4):1761-4.

566 13. Qiang X, Kou Z. Prediction of interspecies transmission for avian influenza A
567 virus based on a back-propagation neural network. Mathematical and Computer
568 Modelling. 2010;52(11–12):2060-5.
569 doi:http://dx.doi.org/10.1016/j.mcm.2010.06.008.

570 14. Wang J, Ma C, Kou Z, Zhou YH, Liu HL. Predicting transmission of avian
571 influenza A viruses from avian to human by using informative physicochemical
572 properties. International journal of data mining and bioinformatics. 2013;7(2):166-79.

573 15. Eng CL, Tong JC, Tan TW. Predicting host tropism of influenza A virus proteins
574 using random forest. BMC medical genomics. 2014;7 Suppl 3:S1. doi:10.1186/1755-
575 8794-7-S3-S1.

576 16. Taubenberger JK, Reid AH, Lourens RM, Wang R, Jin G, Fanning TG.
577 Characterization of the 1918 influenza virus polymerase genes. Nature.
578 2005;437(7060):889-93. doi:10.1038/nature04230.

579 17. Chen GW, Chang SC, Mok CK, Lo YL, Kung YN, Huang JH et al. Genomic
580 signatures of human versus avian influenza A viruses. Emerging infectious diseases.
581 2006;12(9):1353-60. doi:10.3201/eid1209.060276.

582 18. Chen GW, Shih SR. Genomic signatures of influenza A pandemic (H1N1) 2009
583 virus. Emerging infectious diseases. 2009;15(12):1897-903.
584 doi:10.3201/eid1512.090845.

19. Finkelstein DB, Mukatira S, Mehta PK, Obenauer JC, Su X, Webster RG et al. Persistent host markers in pandemic and H5N1 influenza viruses. Journal of virology. 2007;81(19):10292-9. doi:10.1128/JVI.00921-07.

20. Allen JE, Gardner SN, Vitalis EA, Slezak TR. Conserved amino acid markers from past influenza pandemic strains. BMC microbiology. 2009;9:77. doi:10.1186/1471-2180-9-77.

21. Miotto O, Heiny AT, Albrecht R, Garcia-Sastre A, Tan TW, August JT et al. Complete-proteome mapping of human influenza A adaptive mutations: implications for human transmissibility of zoonotic strains. PloS one. 2010;5(2):e9025. doi:10.1371/journal.pone.0009025.

22. Hu YJ, Tu PC, Lin CS, Guo ST. Identification and chronological analysis of genomic signatures in influenza A viruses. PloS one. 2014;9(1):e84638. doi:10.1371/journal.pone.0084638.

23. Pawlak Z. Rough sets. International Journal of Computer and Information Sciences. 1982;11(5):341-56. doi:10.1007/BF01001956.

24. Draminski M, Rada-Iglesias A, Enroth S, Wadelius C, Koronacki J, Komorowski J. Monte Carlo feature selection for supervised classification. Bioinformatics. 2008;24(1):110-7. doi:10.1093/bioinformatics/btm486.

603 25. Bornelov S, Marillet S, Komorowski J. Ciruvis: a web-based tool for rule
604 networks and interaction detection using rule-based classifiers. BMC bioinformatics.
605 2014;15:139. doi:10.1186/1471-2105-15-139.

606 26. Bialas KM, Desmet EA, Takimoto T. Specific residues in the 2009 H1N1 swine-
607 origin influenza matrix protein influence virion morphology and efficiency of viral
608 spread in vitro. PloS one. 2012;7(11):e50595. doi:10.1371/journal.pone.0050595.

609 27. Abed Y, Goyette N, Boivin G. Generation and characterization of recombinant
610 influenza A (H1N1) viruses harboring amantadine resistance mutations.
611 Antimicrobial agents and chemotherapy. 2005;49(2):556-9.
612 doi:10.1128/AAC.49.2.556-559.2005.

613 28. He G, Qiao J, Dong C, He C, Zhao L, Tian Y. Amantadine-resistance among
614 H5N1 avian influenza viruses isolated in Northern China. Antiviral research.
615 2008;77(1):72-6. doi:10.1016/j.antiviral.2007.08.007.

616 29. Cheung CL, Rayner JM, Smith GJ, Wang P, Naipospos TS, Zhang J et al.
617 Distribution of amantadine-resistant H5N1 avian influenza variants in Asia. The
618 Journal of infectious diseases. 2006;193(12):1626-9. doi:10.1086/504723.

619 30. Ilyushina NA, Govorkova EA, Webster RG. Detection of amantadine-resistant
620 variants among avian influenza viruses isolated in North America and Asia. Virology.
621 2005;341(1):102-6. doi:10.1016/j.virol.2005.07.003.

622 31. Khaliq Z, Leijon M, Belak S, Komorowski J. A complete map of potential
623 pathogenicity markers of avian influenza virus subtype H5 predicted from 11
624 expressed proteins. BMC microbiology. 2015;15:128. doi:10.1186/s12866-015-0465-
625 x.

626 32. Bao Y, Bolotov P, Dernovoy D, Kiryutin B, Zaslavsky L, Tatusova T et al. The
627 influenza virus resource at the National Center for Biotechnology Information.
628 Journal of virology. 2008;82(2):596-601. doi:10.1128/jvi.02005-07.

629 33. Edgar R. MUSCLE: multiple sequence alignment with high accuracy and high
630 throughput. Nucleic Acids Research. 2004;32(5):1792-7.

631 34. Draminski M. Michal Dramiski Home Page. 2014.
632 http://www.ipipan.waw.pl/~mdramins/software.htm. Accessed December 10 2014.

633 35. Holm S. A simple sequentially rejective multiple test procedure. Scandinavian
634 journal of statistics. 1979:65-70.

635 36. Bornelov S, Saaf A, Melen E, Bergstrom A, Torabi Moghadam B, Pulkkinen V et
636 al. Rule-based models of the interplay between genetic and environmental factors in
637 childhood allergy. PLoS One. 2013;8(11):e80080. doi:10.1371/journal.pone.0080080.

638 37. Folorunso S, Adeyemo A. Alleviating Classification Problem of Imbalanced
639 Dataset. African Journal of Computing & ICT. 2013;6(2).

640 38. Bekkar M, Alitouche TA. IMBALANCED DATA LEARNING APPROACHES
641 REVIEW. International Journal. 2013.

642 39. Øhrn A, Komorowski J, editors. ROSETTA: A Rough Set Toolkit for Analysis of
643 Data. Proc. Third International Joint Conference on Information Sciences, Fifth
644 International Workshop on Rough Sets and Soft Computing (RSSC'97); 1997 March
645 1-5; Durham, NC, USA.

646 40. Komorowski J. Jan Komorowski's Bioinformatics Lab. 2014.
647 http://bioinf.icm.uu.se/ -> Repositories -> Rosetta. Accessed December 10 2014.

648 41. Komorowski J, Pawlak Z, Polkowski L, Skowron A. Rough sets: A tutorial.
649 Rough fuzzy hybridization: A new trend in decision-making. 1999:3-98.

650 42. Komorowski J. Learning rule-based models - the rough set approach. In: Brahme
651 A, editor. Comprehensive Biomedical Physics Elsevier; 2014.

652 43. Price MN, Dehal PS, Arkin AP. FastTree 2--approximately maximum-likelihood
653 trees for large alignments. PloS one. 2010;5(3):e9490.
654 doi:10.1371/journal.pone.0009490.

655 44. Smeenk CA, Wright KE, Burns BF, Thaker AJ, Brown EG. Mutations in the
656 hemagglutinin and matrix genes of a virulent influenza virus variant, A/FM/1/47-MA,
657 control different stages in pathogenesis. Virus research. 1996;44(2):79-95.

658 45. Liu T, Ye Z. Introduction of a temperature-sensitive phenotype into influenza
659 A/WSN/33 virus by altering the basic amino acid domain of influenza virus matrix
660 protein. Journal of virology. 2004;78(18):9585-91. doi:10.1128/JVI.78.18.9585-
661 9591.2004.

662 46. Watanabe K, Handa H, Mizumoto K, Nagata K. Mechanism for inhibition of
663 influenza virus RNA polymerase activity by matrix protein. Journal of virology.
664 1996;70(1):241-7.

665 47. Akarsu H, Burmeister WP, Petosa C, Petit I, Muller CW, Ruigrok RW et al.
666 Crystal structure of the M1 protein-binding domain of the influenza A virus nuclear
667 export protein (NEP/NS2). The EMBO journal. 2003;22(18):4646-55.
668 doi:10.1093/emboj/cdg449.

669 48. Liu W, Zou P, Ding J, Lu Y, Chen YH. Sequence comparison between the
670 extracellular domain of M2 protein human and avian influenza A virus provides new
671 information for bivalent influenza vaccine design. Microbes and infection / Institut
672 Pasteur. 2005;7(2):171-7. doi:10.1016/j.micinf.2004.10.006.

673 49. Holsinger LJ, Lamb RA. Influenza virus M2 integral membrane protein is a
674 homotetramer stabilized by formation of disulfide bonds. Virology. 1991;183(1):32-
675 43.

676 50. Jackson D, Hossain MJ, Hickman D, Perez DR, Lamb RA. A new influenza virus
677 virulence determinant: the NS1 protein four C-terminal residues modulate
678 pathogenicity. Proceedings of the National Academy of Sciences of the United States
679 of America. 2008;105(11):4381-6. doi:10.1073/pnas.0800482105.

680 51. Heikkinen LS, Kazlauskas A, Melen K, Wagner R, Ziegler T, Julkunen I et al.
681 Avian and 1918 Spanish influenza a virus NS1 proteins bind to Crk/CrkL Src
682 homology 3 domains to activate host cell signaling. The Journal of biological
683 chemistry. 2008;283(9):5719-27. doi:10.1074/jbc.M707195200.

684 52. Min JY, Li S, Sen GC, Krug RM. A site on the influenza A virus NS1 protein
685 mediates both inhibition of PKR activation and temporal regulation of viral RNA
686 synthesis. Virology. 2007;363(1):236-43. doi:10.1016/j.virol.2007.01.038.

687 53. Hale BG, Kerry PS, Jackson D, Precious BL, Gray A, Killip MJ et al. Structural
688 insights into phosphoinositide 3-kinase activation by the influenza A virus NS1
689 protein. Proceedings of the National Academy of Sciences of the United States of
690 America. 2010;107(5):1954-9. doi:10.1073/pnas.0910715107.

691 54. Hale BG, Jackson D, Chen YH, Lamb RA, Randall RE. Influenza A virus NS1
692 protein binds p85beta and activates phosphatidylinositol-3-kinase signaling.
693 Proceedings of the National Academy of Sciences of the United States of America.
694 2006;103(38):14194-9. doi:10.1073/pnas.0606109103.

695 55. Melen K, Kinnunen L, Fagerlund R, Ikonen N, Twu KY, Krug RM et al. Nuclear
696 and nucleolar targeting of influenza A virus NS1 protein: striking differences between
697 different virus subtypes. Journal of virology. 2007;81(11):5995-6006.
698 doi:10.1128/JVI.01714-06.

699 56. Pan C, Cheung B, Tan S, Li C, Li L, Liu S et al. Genomic signature and mutation
700 trend analysis of pandemic (H1N1) 2009 influenza A virus. PloS one.
701 2010;5(3):e9549. doi:10.1371/journal.pone.0009549.

702 57. Tamuri AU, Dos Reis M, Hay AJ, Goldstein RA. Identifying changes in selective
703 constraints: host shifts in influenza. PLoS computational biology.
704 2009;5(11):e1000564. doi:10.1371/journal.pcbi.1000564.

705 58. Lipatov AS, Yen HL, Salomon R, Ozaki H, Hoffmann E, Webster RG. The role
706 of the N-terminal caspase cleavage site in the nucleoprotein of influenza A virus in
707 vitro and in vivo. Archives of virology. 2008;153(3):427-34. doi:10.1007/s00705-
708 007-0003-8.

709 59. Bussey KA, Desmet EA, Mattiacio JL, Hamilton A, Bradel-Tretheway B, Bussey
710 HE et al. PA residues in the 2009 H1N1 pandemic influenza virus enhance avian
711 influenza virus polymerase activity in mammalian cells. Journal of virology.
712 2011;85(14):7020-8. doi:10.1128/JVI.00522-11.

713 60. Desmet EA, Bussey KA, Stone R, Takimoto T. Identification of the N-terminal
714 domain of the influenza virus PA responsible for the suppression of host protein
715 synthesis. Journal of virology. 2013;87(6):3108-18. doi:10.1128/JVI.02826-12.

716 61. Jin H, Lu B, Zhou H, Ma C, Zhao J, Yang CF et al. Multiple amino acid residues
717 confer temperature sensitivity to human influenza virus vaccine strains (FluMist)
718 derived from cold-adapted A/Ann Arbor/6/60. Virology. 2003;306(1):18-24.

719 62. Xu C, Hu WB, Xu K, He YX, Wang TY, Chen Z et al. Amino acids 473V and
720 598P of PB1 from an avian-origin influenza A virus contribute to polymerase activity,
721 especially in mammalian cells. The Journal of general virology. 2012;93(Pt 3):531-
722 40. doi:10.1099/vir.0.036434-0.

723 63. Mehle A, Doudna JA. Adaptive strategies of the influenza virus polymerase for
724 replication in humans. Proceedings of the National Academy of Sciences of the
725 United States of America. 2009;106(50):21312-6. doi:10.1073/pnas.0911915106.

726 64. Yamada S, Hatta M, Staker BL, Watanabe S, Imai M, Shinya K et al. Biological
727 and structural characterization of a host-adapting amino acid in influenza virus. PLoS
728 pathogens. 2010;6(8):e1001034. doi:10.1371/journal.ppat.1001034.

729 65. Bussey KA, Bousse TL, Desmet EA, Kim B, Takimoto T. PB2 residue 271 plays
730 a key role in enhanced polymerase activity of influenza A viruses in mammalian host
731 cells. Journal of virology. 2010;84(9):4395-406. doi:10.1128/JVI.02642-09.

732 66. Foeglein A, Loucaides EM, Mura M, Wise HM, Barclay WS, Digard P. Influence
733 of PB2 host-range determinants on the intranuclear mobility of the influenza A virus
734 polymerase. The Journal of general virology. 2011;92(Pt 7):1650-61.
735 doi:10.1099/vir.0.031492-0.

736 67. Conenello GM, Zamarin D, Perrone LA, Tumpey T, Palese P. A single mutation
737 in the PB1-F2 of H5N1 (HK/97) and 1918 influenza A viruses contributes to
738 increased virulence. PLoS pathogens. 2007;3(10):1414-21.
739 doi:10.1371/journal.ppat.0030141.

740 68. Burke DF, Smith DJ. A recommended numbering scheme for influenza A HA
741 subtypes. PloS one. 2014;9(11):e112302. doi:10.1371/journal.pone.0112302.

742 69. Caton AJ, Brownlee GG, Yewdell JW, Gerhard W. The antigenic structure of the
743 influenza virus A/PR/8/34 hemagglutinin (H1 subtype). Cell. 1982;31(2 Pt 1):417-27.

744 70. Brownlee GG, Fodor E. The predicted antigenicity of the haemagglutinin of the
745 1918 Spanish influenza pandemic suggests an avian origin. Philosophical transactions
746 of the Royal Society of London Series B, Biological sciences. 2001;356(1416):1871-
747 6. doi:10.1098/rstb.2001.1001.

748

749 Figure Legends

750 **Figure 1. Mean accuracies of the classifiers from 10-fold cross validations.** The
751 red bars are for the H1N1 subtype and cyan bars are for the H3N2 subtype.
752 **Figure 2. Performance of the rule-based models.** The figure shows how well the
753 models perform from a classification point of view, which is shown in terms of
754 Mathew's correlation coefficient (MCC) values when tested on its corresponding
755 complete input data set for each protein model of both subtypes. A value of 1 means a
756 perfect classification, 0 is for a prediction no better than random and -1 indicates a

757 total disagreement between predictions and observations. The red bars are for the
758 H1N1 subtype and cyan bars are for the H3N2 subtype.

759 **Figure 3. Ciruvis diagrams of combinations from the rules of H1N1 models.**
760 Models having at least three combinations are shown. The outer circle shows the
761 positions. The inner circle shows the position or positions to which the position of the
762 outer circle is connected. The edges show these connections. The width and color of
763 the edges are related to the connection score (low = yellow and thin, high = red and
764 thick). The width of an outer position is the sum of all connections to it, scaled so that
765 all positions together cover the whole circle [25].

766 **Figure 4. Ciruvis diagrams of combinations from the rules of H3N2 models.**
767 Models having at least three combinations are shown. The outer circle shows the
768 positions. The inner circle shows the position or positions to which the position of the
769 outer circle is connected. The edges show these connections. The width and color of
770 the edges are related to the connection score (low = yellow and thin, high = red and
771 thick). The width of an outer position is the sum of all connections to it, scaled so that
772 all positions together cover the whole circle [25].

773 **Figure 5. Phylogeny of PB2 H3N2 protein of avian hosts annotated with top 5**
774 **avian rules form the PB2 H3N2 model.** Each sequences is represented by its
775 GeneBank accession. The violet nodes mark the sequences that supports rule 1,2,3,4
776 and 5, which are 91.4% of the total sequences. Similarly the DarkViolet nodes mark
777 the sequences that support rule 1, 2, 3 and 4 but lacks support for rule 5, which are
778 2.2% of the total sequences. The nodes with a LightBlue background are the new,
779 unseen sequences. The unmarked nodes do not support the top 5 rules, and were
780 either supporting rules other than the top 5 or were not classified by the models.

Additional Files

Additional file 1: This file contains the lists of significant features that were selected by MCFS for all the proteins of both subtypes.

Format: XLSX, Size: 75Kb

Additional file 2: This file contains the rule-based models for all the proteins of both subtypes.

Format: XLSX, Size: 42Kb

Additional file 3: This file contains list of names of the unseen viral sequences for both subtypes that were either miss-classified or could not be classified by the rule-based models.

Format: XLSX, Size: 11Kb

Additional file 4: This file contains singular and combinatorial signatures from the rules for both subtypes.

Format: XLSX, Size: 75Kb

Additional file 5: This file contains all the phylogeny trees marked with top 5 rules. Each sequences is represented by its GeneBank accession. The nodes with a LightBlue background are the new, unseen sequences. The unmarked nodes do not support the top 5 rules, and were either supporting rules other than the top 5 or were not classified by the models.

Format: PDF, Size: 7.3Mb

Tables

Table 1: The training data.

	Nr. of sequences for each subtype						
	H1N1		H3N2			Features after MCFS	
Protein	Avian	Human	Avian	Human	Total Features	H1N1	H3N2
HA	214	5205	164	3715	628	115	88
NA	205	3093	173	3412	517	93	79
NS1	150	1258	150	1176	249	98	85
NEP	61	407	54	299	124	31	26
NP	125	839	93	773	506	61	69
M1	45	467	42	355	275	18	15
M2	65	461	64	503	98	25	23
PA	192	1677	143	1358	726	65	47
PA-X	57	164	45	244	252	28	24
PB1	171	1654	132	1347	762	59	33
PB2	184	1817	136	1297	776	52	42
PB1-F2	151	224	112	737	101	64	54

Table 2: Rule-based model of HA protein for the H1N1 subtype

Rule	Accuracy (%)	Support	Decision Coverage (%)
IF P435=I THEN host=Human	99.9	5128	98.4
IF P200=S THEN host=Human	99.9	4052	77.8
IF P10=Y THEN host=Human	99.8	3998	76.7
IF P88=S THEN host=Human	99.9	3989	76.5
IF P6=V THEN host=Human	99.8	3936	75.5
IF P222=R THEN host=Human	99.9	3823	73.4
IF P220=T THEN host=Human	100.0	3584	68.8
IF P516=K THEN host=Human	99.9	1818	34.9
IF P200=P and P222=K THEN host=Avian	91.3	229	97.7
IF P130=K THEN host=Avian	91.3	218	93.0
IF P2=E and P222=K THEN host=Avian	96.2	208	93.5
IF P137=A and P544=L THEN host=Avian	96.1	205	92.1
IF P78=L and P435=V THEN host=Avian	97.1	204	92.5
IF P9=F THEN host=Avian	98.5	204	93.9
IF P6=F THEN host=Avian	98.2	169	77.6
IF P14=V THEN host=Avian	99.4	165	76.6
IF P173=T THEN host=Avian	98.7	158	72.9

805 **Table 3: Performance of the rule-based models on the new, unseen data**

	Human Sequences		Avian Sequences	
Protein	**Total**	**Correctly classified**	**Total**	**Correctly classified**
HA-H1N1	107	104	2	2
HA-H3N2	72	72	4	4
M1-H1N1	24	24	0	0
M1-H3N2	7	7	0	0
M2-H1N1	30	26	1	1
M2-H3N2	21	15	3	3
NA-H1N1	32	32	2	1
NA-H3N2	45	45	4	3
NP-H1N1	13	13	1	1
NP-H3N2	7	7	4	4
NS1-H1N1	30	30	2	2
NS1-H3N2	18	18	3	3
NEP-H1N1	11	11	2	2
NEP-H3N2	7	7	2	2
PAX-H1N1	17	13	2	2
PAX-H3N2	6	6	0	0
PA-H1N1	33	28	2	2
PA-H3N2	23	23	3	3
PB1F2-H1N1	2	2	2	2
PB1F2-H3N2	8	7	4	0
PB1-H1N1	27	27	0	0
PB1-H3N2	19	19	1	1
PB2-H1N1	28	28	2	2
PB2-H3N2	15	15	3	3

806

807 **Table 4: Amino acid residues having the most interactions in the models of both subtypes.**

Subtype	**Protein**	**Positions**	**Number of interactions**
H1N1	HA	222K	2
	M1	121T	5
	M2	14G	6
	NEP	57S, 60S	2
	PA	28P, 277S	3
	PA-X	28P	4
	PB1	179M, 741A	3
	PB2	65E	3
H3N2	M1	101R	2
	M2	11T, 14G, 31S, 54R	2
	NEP	14M	4
	PB1	212L	2
	PB2	82N	6

808

809 **Table 5: Novel singular aa positions associated to host adaptation**

Protein	**Novel singular positions**
HA	6,9,10,14,23,47,66,69,78,88,91,94,130,173,189,200,220,222,435,516
M1	30,116,142,207,209
M2	13,16,31,36,43,51,54
NA	16,18,19,23,30,40,42,44,46,47,74,79,147,150,157,166,232,285,341,344,351,369,372, 389,397,435,437,466
NP	31,53,98,146,444,450,498
NS1	6,7,14,23,27,28,74,123,152,192,220,226
NS2	6,7,14,32,34,48,83,86
PA	85,323,336,348,362,300

PAX	28,85,210,233
PB1	12,54,59,113,175,212,339,435,576,586,587,619,709
PB1F2	3,6,12,17,21,25,26,27,28,33,47,52,54,57,58,60,62,65,82
PB2	54,65,354

Table 6: Amino acid changes associated with host adaptation

H1N1				**H3N2**			
Protein	**Position**	**Avian**	**Human**	**Protein**	**Position**	**Avian**	**Human**
HA	6	F	V	HA	78	R	E
NA	46	P	T	NA	30	A	I
	74	L	V		40	N	Y
NP	100	R	I,V		44	I	S
NS1	6	I	M	NP	16	G	D
NEP	6	I	M	PA-X	28	P	L
PB1-F2	58	L	-	PA	28	P	L
PB2	588	A	I		57	R	Q
				PB2	9	D	N
					64	M	T

Table 7: Performance of the H1N1 models on H3N2 data and vice versa. Sensitivity is the ability to correctly predict human sequences and specificity is the ability to correctly predict avian sequences where 1 means perfect prediction and 0 means no correct predictions. Mathew's correlation coefficient (MCC) value is a measure of how well the model performs overall where 1 is perfect prediction, 0 is similar to prediction by chance and -1 is total disagreement between observations and predictions. "na" means the measure could not be calculated for the given model.

	Protein	**Sensitivity**	**Specificity**	**MCC**
H3N2 data - H1N1 models	HA	1	0	na
	M1	1	0.895	0.941
	M2	1	0.742	0.848
	NA	1	0	na
	NP	1	0.891	0.938
	NS1	1	0.745	0.849
	NEP	1	0.642	0.776
	PA-X	0	1	na
	PA	0.021	0.93	-0.11
	PB1-F2	0.023	1	0.056
	PB1	0.563	0.909	0.302
	PB2	0.979	0.949	0.873
H1N1 data - H3N2 models	HA	0	na	na
	M1	0.957	0.975	0.885
	M2	0.987	0.766	0.804
	NA	1	0	-0.004
	NP	0.363	0.984	0.251
	NS1	0.365	0.993	0.236
	NEP	0.027	1	0.06
	PA-X	0.202	0.982	0.224
	PA	0.247	0.995	0.177
	PB1-F2	0.991	0.804	0.831
	PB1	0.992	0.877	0.888
	PB2	0.956	0.951	0.788

820 **Table 8: Amino acid positions discussed in literature from the models of both the subtypes for all**

821 **proteins**

Protein	Positions	Description
M1	115,121,137	Known signatures of host-adaptation [18, 21, 22]
	30,142,207,209	Affecting viral production on mutation [26]
	121	Affecting viral replication [44]
	101	Determinant of temperature sensitivity [45], located in a transcription inhibition site [46] and is also interacting with NEP [47]
M2	11,14,18,20,28, 55,57,78,82,89, 93	Known signatures of host-adaptation [18, 21, 22, 48]
	31	S31N is a known marker for amantadine resistance [27-30]
	18,20	Lie next to 17,19 which forms a di-sulphide bond [49]
NS1	18,21,22,53,60, 70,81,112,114,1 71,215,227	Known signatures of host-adaptation [19, 50, 17, 21, 22, 20]
	215	Required for Crk/CrL-SH3 binding [51]
	123	Necessary for interaction with PKR, resulting in an inhibition of eIF2alpha phosphorylation [52]
	95	Along with others, has been shown to be necessary for binding p85beta and activating PI3K signaling [53, 54]
	220	Part of nuclear localization signal 2 essential for the importin-alpha binding [55]
NEP(NS2)	57,60,70,107	Known signatures of host-adaptation [17, 56, 18, 22, 21]
NP	16,33,100,214,2 83,313,351,353, 357,422	Known signatures of host-adaptation [20, 18, 57, 19, 22, 21]
	16	D16G shown to decrease pathogenicity several fold [58]
PA	28,55,57,65,256 ,268,277,356,38 2,400,409	Known signatures of host-adaptation [19, 18, 20, 57, 22, 21]
	85,336	Residues 85I and 336M are deemed important for enhanced polymerase activity in mammalian cells [59]
	57,65,85	Shown to be involved in suppressing the host cell protein synthesis during infection [60]
PB1	52,179,216,298, 327,336,361,37 5,581,741	Known signatures of host-adaptation [57, 18, 21, 22, 16]
	581	Shown to be conferring temperature sensitivity to human influenza virus vaccine strains [61]
	473	Mutation at position 473 has been shown to decrease polymerase activity [62]
PB2	9,44,64,81,105, 271,292,368,45 3,588,613,682,6 84	Known signatures of host-adaptation [57, 18, 19, 22, 21]
	591	591Q is known to mimic the effect of 627K [63, 64]
	271	271A shown to increase polymerase activity in mammalian cells [65]
	271,588	Also been shown to be host range determinants [66]
PB1-F2	16,23,42,66,70, 73,76	Known signatures of host-adaptation [17, 22]
	66	Linked with affecting pathogenicity [67]
NA	46,47,74,147,15	Under selection pressure with a shift of hosts from birds

	7,341,351	to humans [57]
	344	Calcium ion binds here that stabilizes the molecule (UniProt: Q9IGQ6).
HA	2,6,9,10,14	Signal peptide domain
	88,173,220,22	Position 71, 159, 206 and 208 of the fully-mature HA with H3-numbering [68]) are part of the antigenic sites Cb, Sb and Ca of the HA protein, respectively [69, 70]

822

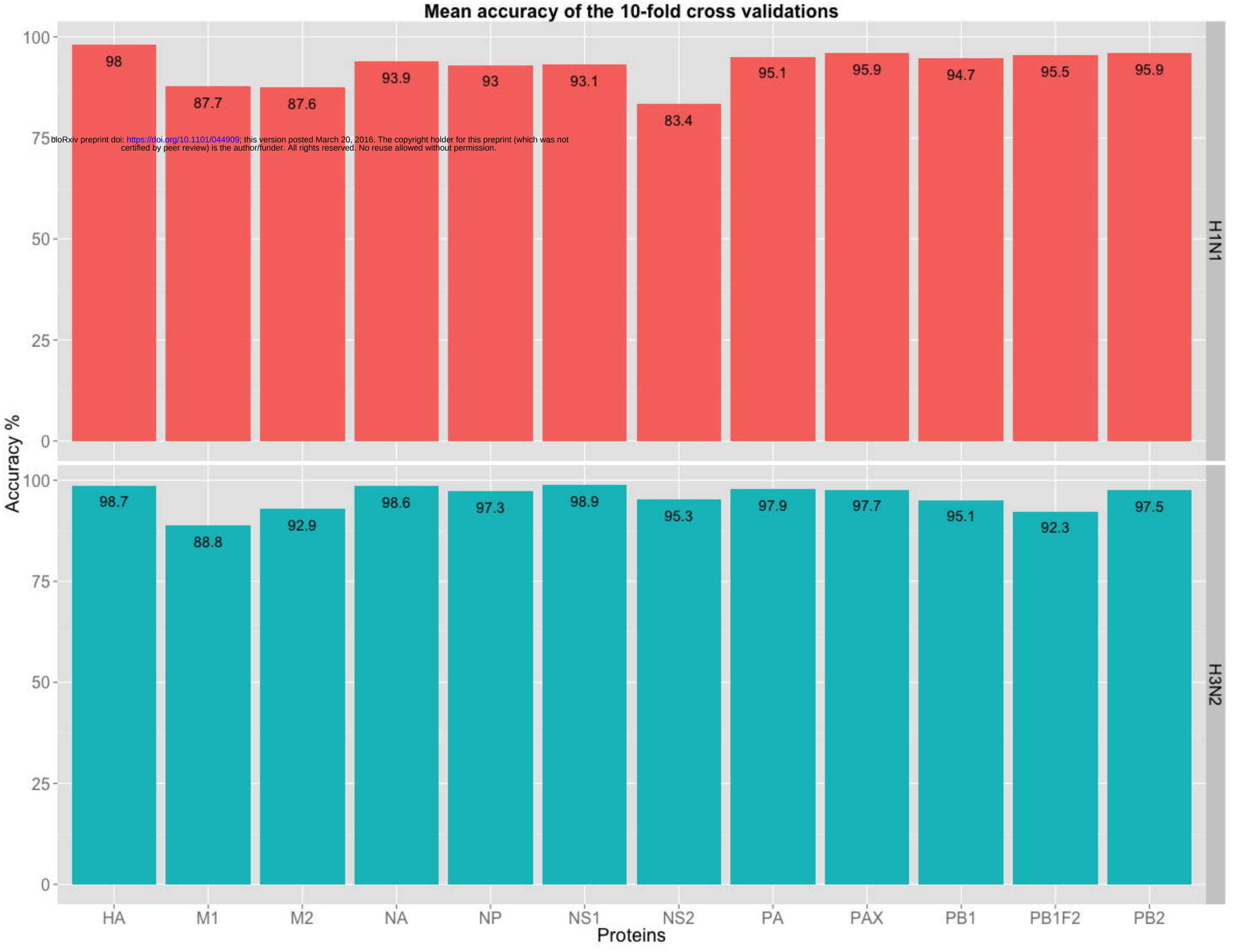

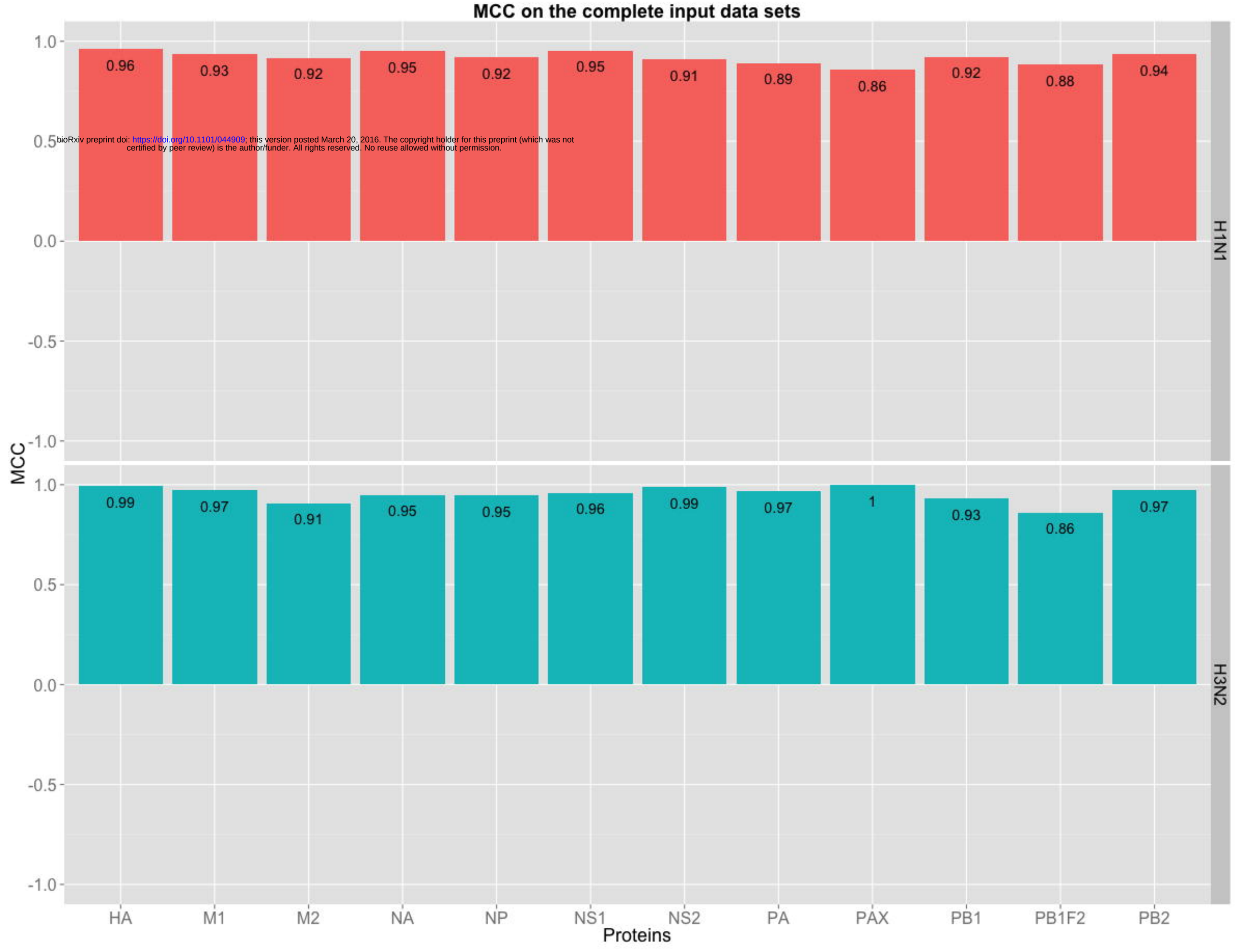

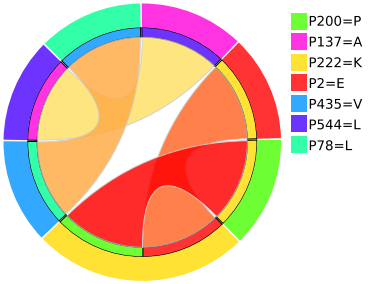

HA

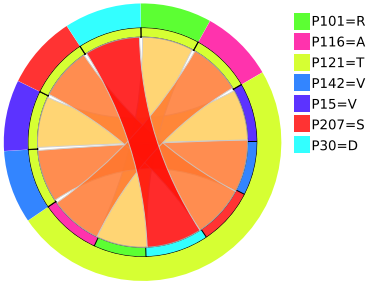

M1

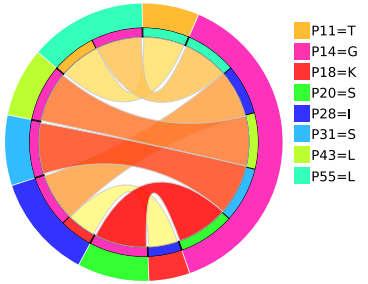

M2

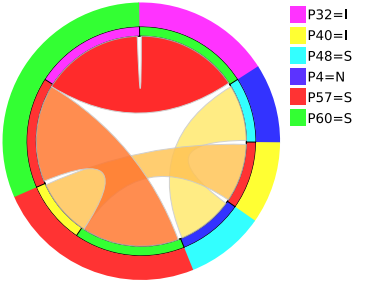

NEP

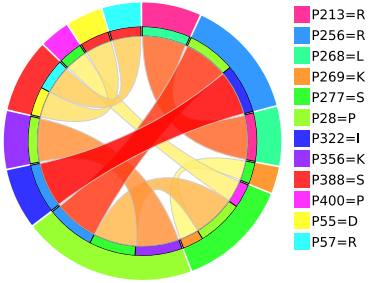

PA

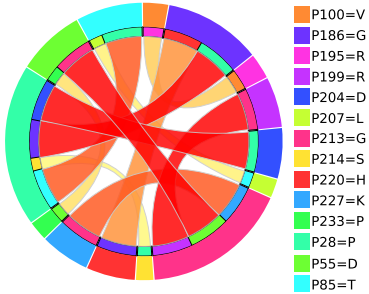

PA-X

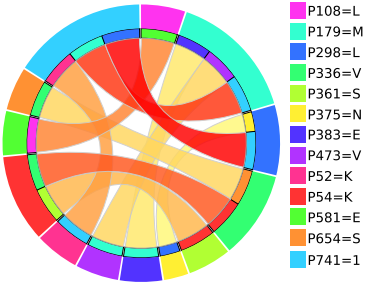

PB1

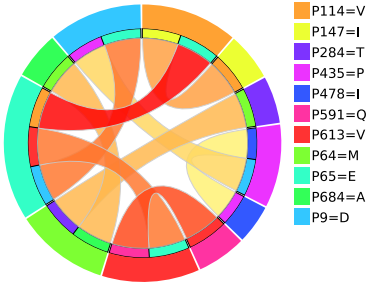

PB2

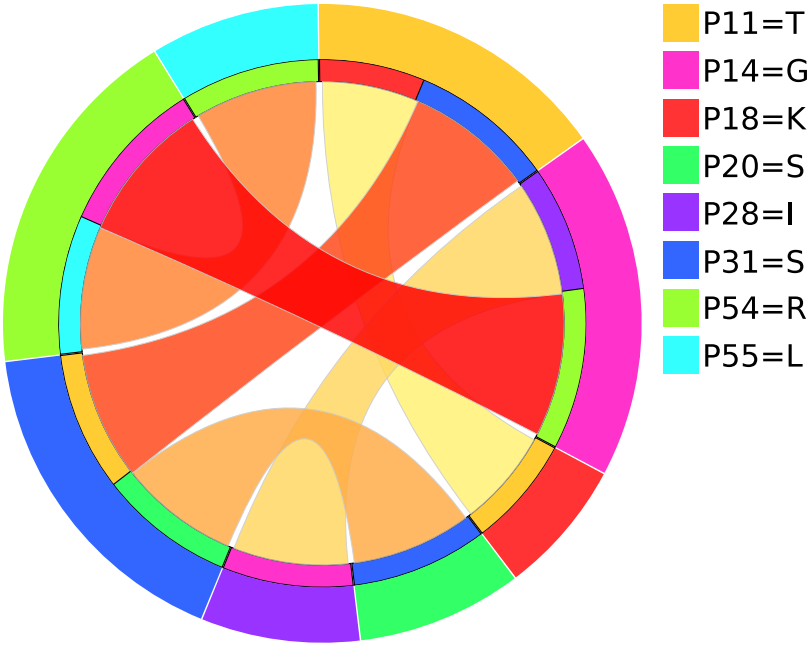

M2

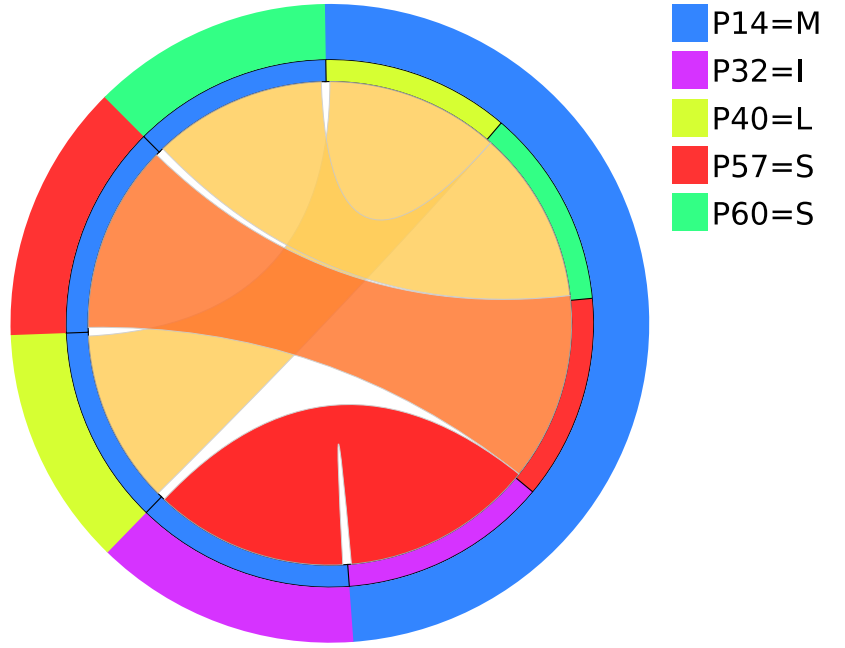

NEP

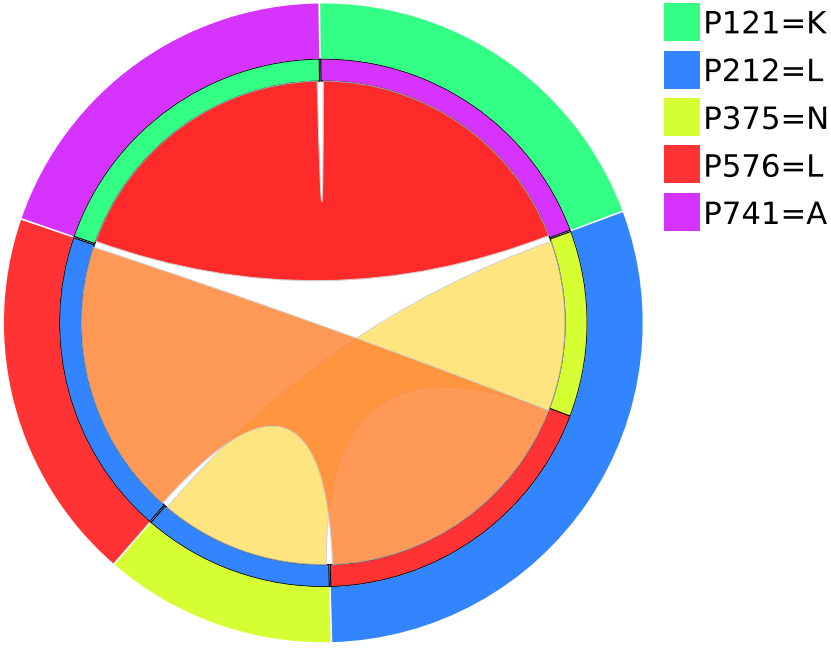

PB1

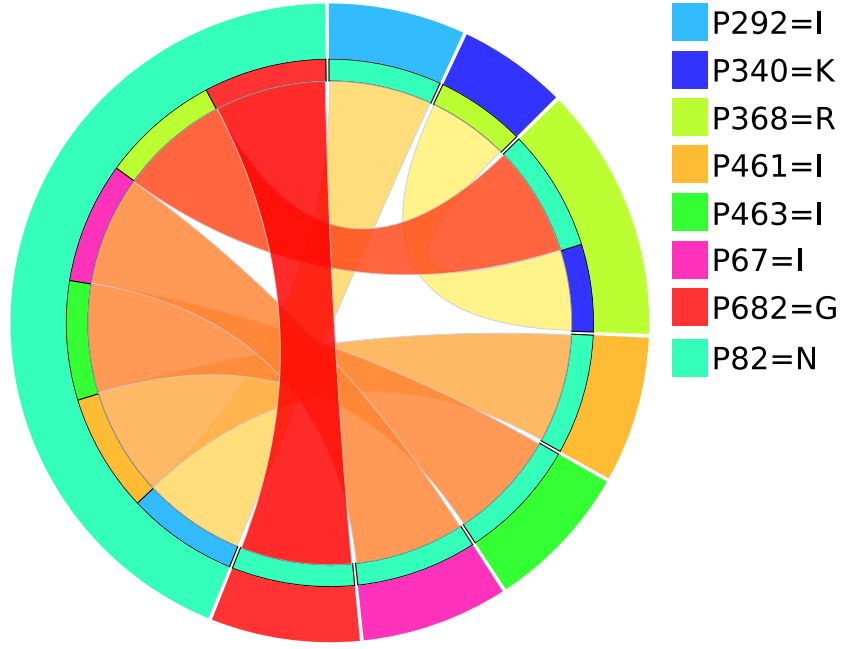

PB2

PB2_H3N2_Avian.tree
1,2,3,4,5 apply, 91.4% coverage
1,2,3,4,5 apply, 1.8% coverage
1,2,3,4,5 apply, 2.2% coverage
1,2,3,4,5 apply, 2.2% coverage
1,2,3,4,5 apply, 1.4% coverage
AACT74605
AAC82455
AAC82553
AGL59869
AAB61781
AAC82449
AGL62479
AHL83702
AEL82930
AAC82474
AGR54574
AGR54573
AGR54575
ACS55590
AAN92049
AAL80621
AAC73151
ACN86434
AGK42361
AAC82534
ACN55843
AAN92809
AAC82158
AAP27622
ACF21954
AAC82511
AAN94823
AAN94822
AAC82529
AAC73939
AAC82504
AAC82511
AAL58111
AGB94850
ACG23601
AAT26946
AAN92091
AAN92092
AEB35816
AFN66839
AEM77705
AAL24594
AHN81766
AAC82559
AAC82560
AGK78955
AAC82558
AEB94468
AAC82557
AAC82576
AAC82573
AAC82562
AEA76945
AAC82561
AEA76943
AAN93396
AAB19756
AAC82564
AAC82565
AAN93435
AAC82566
AAL24594
AAL24594
AEA76797
AAA42771
AAC82567
AAC82568
AAN93227
AAC82569
AAN93228
AAC82570
AAL11972
AAB20324
AAU10985
AAL11997
BAC55919
AAC82571
AAC82572
AHB90540
AAC82573
AAN92474
AAC14496
AAC11550
AAC82574
AAN93228
AAB67828
AGL59971
AEP77004
AAZ76516
AEP77293
AAB34185
AAC82575
ACD86838
AAC82539
AAL81660
AAL81719
AAC82539
AAC82523
AAC82538
AAL82535
AAN17923
AAC82527
AAC73971
AAC82487
AAC82542
AAC82543
AAC82540
AAC82541
AAN94233
AAN94234
AAN94235
AAC82544
AAC73934
AAC82545
AAN93355
AHL81856
AAC82546
AAN93431
AAC82547
AAN94129
AAC82548
AAC82549
AAC73937
AAC82550
AAC82551
AAC82552
AAC82553
AAC82554
AAC82555
AAC82556
AAC82557
AAC82576
AAC82573
AAC82562
AEA76945
AAN93396
AAB19756
AAC82564
AAC82565
AAN93435
AAC82566